Journal of Systems Engineering and Electronics
Vol. 33, No. 2, April 2022, pp.322 – 329

A method of Robust low-angle target height and compound reflection coefficient joint estimation

WANG Shenghua[1,2,*], CAO Yunhe[3], and LIU Yutao[2]

1. School of Communications and Information Engineering, Xi'an University of Posts and Telecommunications, Xi'an 710061, China; 2. Science and Technology on Communication Networks Laboratory, Shijiazhuang 050081, China;
3. National Laboratory of Radar Signal Processing, Xidian University, Xi'an 710071, China

Abstract: It is always a challenging issue for radar systems to estimate the height of a low-angle target in the multipath propagation environment. The highly deterministic maximum likelihood estimator has a high accuracy, but the errors of the ground reflection coefficient and the reflecting surface height have serious influence on the method. In this paper, a robust estimation method with less computation burden is proposed based on the compound reflection coefficient multipath model for low-angle targets. The compound reflection coefficient is estimated from the received data of the array and then a one-dimension generalized steering vector is constructed to estimate the target height. The algorithm is robust to the reflecting surface height error and the ground reflection coefficient error. Finally, the experiment and simulation results demonstrate the validity of the proposed method.

Keywords: low-angle target, robust joint estimation, compound reflection coefficient, multipath, direction of arrival (DOA).

DOI: 10.23919/JSEE.2022.000033

1. Introduction

Modern fighters often use the radar blind zone and the multipath effect to carry out low-altitude attack [1−6]. In this case, the ground clutter and multipath echo reduce the radar measurement and tracking performance. For a low-angle target, the direct-wave signal and the multipath-signals enter the main lobe of the radar beam almost at the same time [7−10], but the phase difference of the direct-wave and the multipath-wave changes sharply with the target's height or range. As a consequence, the amplitude of the received echo of radar changes acutely [11−15].

At present, array super-resolution technology is often used to solve the problem of low-angle target height estimation [16−18]. Subspace-based direction of arrival (DOA) estimation algorithms such as the multiple signal classification (MUSIC) algorithm [19,20] and the estimation of signal parameters via rotational invariance techniques (ESPRIT) [21−24] algorithm cannot be used to deal with low-angle estimation, because the direct signal and the multipath reflected signals are coherent. Although the coherence between the direct signal and the multipath reflected signals can be removed by the spatial smoothing technique [25], the equivalent array aperture after spatial smoothing becomes obviously shorter and the accuracy of the low-angle target height estimation is comparatively degraded. The maximum likelihood (ML) estimation [26−28] method is a frequently used parameter estimation algorithm to deal with coherent sources without loss of aperture. However, high computation cost for multi-targets limits its application in practice. When the incident angle of the direct wave signal is less than one fourth of the beam-width, the performance of the aforementioned methods will decrease sharply. Additionally, these methods do not make use of the geometric relationship between the incident angles of the direct wave and the multipath reflected wave. The estimation accuracy of these methods is not high enough to meet the needs of the high-precision measurement radar.

The highly deterministic ML estimator [29−31] has a high accuracy for target height estimation. Based on the assumption that the ground reflection coefficient, the radar height, and the target distance have been known accurately, it defines a single steering vector of the specular multipath propagation model. In fact, the ground reflection coefficient is difficult to be obtained in advance and it is a varying parameter. It changes with the incident angle, the ground surface condition, and the polarization mode of radar. Moreover, the highly deterministic ML estimator also considers the reflecting surface height the same as the altitude of the ground where the radar is erec-

Manuscript received January 13, 2021.
*Corresponding author.
This work was supported by the National Natural Science Foundation of China (61771367) and the Science and Technology on Communication Networks Laboratory (6142104190204).

ted. However, the reflecting point is random and varying and the reflecting surface height cannot always be a constant. When there are some errors of the reflecting surface height or the ground reflection coefficient, the measurement accuracy of the highly deterministic ML estimator will drop dramatically.

In this paper, a robust method for the joint estimation of the low-angle target height and the compound reflection coefficient is proposed based on the compound reflection coefficient multipath model. The proposed method uses the echo data to estimate the compound reflection coefficient, and then utilizes the geometric relationship between the target and the multipath image to set up a one-dimension generalized steering vector. The proposed method has low computational burden for its one-dimension search. It is also insensitive to the ground reflection coefficient error and the reflecting surface height error. This paper is organized as follows: Section 2 gives a low-angle target receiving model of array radar in a multipath environment. In Section 3, the proposed method is described in detail. In Section 4, the experiment results and simulation data demonstrate the validity of the proposed method. Finally, Section 5 concludes this paper.

2. Multipath signal model

The flat-earth multipath low-angle model is shown in Fig. 1. The incident angles of the multipath signals received by each element are approximately equal. This situation can be approximately described by a multipath reflection model passing through the same reflecting point shown in Fig. 1.

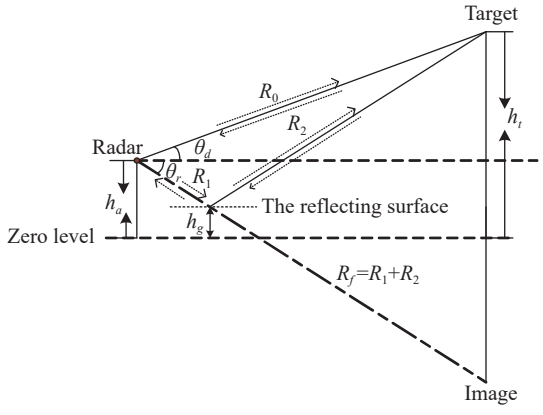

Fig. 1 Flat-earth multipath low-angle model

The criterion of flat-earth [32] is

$$\sigma_h < \frac{\lambda}{8\sin\psi} \tag{1}$$

where σ_h is the variance of the ground surface relief according to Gauss distribution, λ is the wavelength, and ψ is the grazing angle. The wavelength of meter band radar is long and the grazing angle of the low-angle target is very small. Thus the ground surface with little surface relief can be approximated to the flat-earth model.

Suppose the radar is a uniform linear multichannel digital array radar with N elements. It is a meter band, horizontally polarized radar, and its inter-element distance is d. The radar receives the direct signal from the low-angle target and the reflected signal from the reflecting surface. R_1 and R_2 are the distances from the radar to the reflector and from the reflector to the target respectively. The incident angles of the direct signal and the reflected signal are θ_d and θ_r, respectively. The antenna center height of the radar is h_a. The heights of the reflecting surface and the target are h_g and h_t, respectively. The direct distance from the low-angle radar to the target is R_0 and the distance from the low-angle radar to the mirror image is R_f.

In this paper four echo paths are considered. The first echo path is that the signal goes straight from the radar antenna to the target and returns straight from the target to the radar antenna. The second echo path is that the signal goes straight from the radar antenna to the target and returns from the target to the radar antenna via the reflecting surface. The third echo path is that the signal goes to the target via the reflecting surface and returns straight to the radar antenna. The fourth echo path is that the signal goestothetargetviathereflectingsurfaceandsodoesthereturn.

For narrowband signal mode, the signal emitted by radar is

$$s(t) = g(t)\mathrm{e}^{\mathrm{j}(2\pi f_0 t+\varphi)} \tag{2}$$

where f_0 is the frequency of the electromagnetic wave emitted, and φ is the initial phase, and $g(t)$ is the complex amplitude.

Suppose that the radar cross section (RCS) of the target is the same for the above four beam irradiation paths. The signals received by radar are

$$y(t) = P(\theta_d)s(t-\tau_0) + P(\theta_d)\rho s\left(t-\tau_0-\frac{2\Delta R}{\mathrm{c}}\right) + P(\theta_r)\rho s\left(t-\tau_0-\frac{2\Delta R}{\mathrm{c}}\right) + P(\theta_r)\rho^2 s\left(t-\tau_0-\frac{4\Delta R}{\mathrm{c}}\right) + w(t) \tag{3}$$

where τ_0 is the time delay from the target to the radar antenna center and $\tau_0 = 2R_0/c$. $w(t)$ is the Gaussian white noise of the receiver. c is the propagation velocity of electromagnetic wave. ρ is the ground specular reflection coefficient. $P(\theta_d)$ and $P(\theta_r)$ are the normalized antenna gains in the direction of the direct wave and the reflected wave, respectively. ΔR is the distance difference between the target and the image arriving at the radar. When $R_0 \gg h_a$ and $R_0 \gg h_t$ [21], the following equation holds:

$$\Delta R = R_f - R_0 \approx \frac{2(h_f - h_g)(h_a - h_g)}{R_0}. \tag{4}$$

For a low-angle target, both the direct-wave and the multipath reflected waves are in the main lobe of the beam, and it can be considered approximately that

$$P(\theta_d)=P(\theta_r)=\xi. \tag{5}$$

The receiving signal of the nth $(n=1,2,\cdots,N)$ element can be written as

$$\begin{aligned}x_n(t)=&\xi s\left(t-\left(\tau_0-\frac{(n-1)d\sin\theta_d}{\mathrm{c}}\right)\right)+\\&\xi\rho\mathrm{e}^{-\mathrm{j}\frac{2\pi\Delta R}{\lambda}}s\left(t-\left(\tau_0-\frac{(n-1)d\sin\theta_d}{\mathrm{c}}\right)\right)+\\&\xi\rho\mathrm{e}^{-\mathrm{j}\frac{2\pi\Delta R}{\lambda}}s\left(t-\left(\tau_0-\frac{(n-1)d\sin\theta_r}{\mathrm{c}}\right)\right)+\\&\xi\rho^2\mathrm{e}^{-\mathrm{j}\frac{4\pi\Delta R}{\lambda}}s\left(t-\left(\tau_0-\frac{(n-1)d\sin\theta_r}{\mathrm{c}}\right)\right)+w_n(t)\end{aligned} \tag{6}$$

where λ is the wavelength of the electromagnetic wave. $w_n(t)$ is a Gauss white noise uncorrelated to the direct wave signal and the reflected wave signals.

Substituting (2) into (6), we have

$$\begin{aligned}x_n(t)=&\xi g(t-\tau_0)\mathrm{e}^{\mathrm{j}\left(2\pi f_0\left(t-\left(\tau_0-\frac{d_n\sin\theta_d}{\mathrm{c}}\right)\right)+\varphi\right)}+\\&\xi\rho\mathrm{e}^{-\mathrm{j}\frac{2\pi\Delta R}{\lambda}}g(t-\tau_0)\mathrm{e}^{\mathrm{j}\left(2\pi f_0\left(t-\left(\tau_0-\frac{d_n\sin\theta_d}{\mathrm{c}}\right)\right)+\varphi\right)}+\\&\xi\rho\mathrm{e}^{-\mathrm{j}\frac{2\pi\Delta R}{\lambda}}g(t-\tau_0)\mathrm{e}^{\mathrm{j}\left(2\pi f_0\left(t-\left(\tau_0-\frac{d_n\sin\theta_r}{\mathrm{c}}\right)\right)+\varphi\right)}+\\&\xi\rho^2\mathrm{e}^{-\mathrm{j}\frac{4\pi\Delta R}{\lambda}}g(t-\tau_0)\mathrm{e}^{\mathrm{j}\left(2\pi f_0\left(t-\left(\tau_0-\frac{d_n\sin\theta_r}{\mathrm{c}}\right)\right)+\varphi\right)}+\\&w_n(t)=\left(1+\rho\mathrm{e}^{-\mathrm{j}\frac{2\pi\Delta R}{\lambda}}\right)s'(t)a_n(\theta_d)+\\&\rho\mathrm{e}^{-\mathrm{j}\frac{2\pi\Delta R}{\lambda}}\left(1+\rho\mathrm{e}^{-\mathrm{j}\frac{2\pi\Delta R}{\lambda}}\right)s'(t)a_n(\theta_r)+w_n(t)=\\&\left(1+\rho\mathrm{e}^{-\mathrm{j}\frac{2\pi\Delta R}{\lambda}}\right)s'(t)\left(a_n(\theta_d)+\rho\mathrm{e}^{-\mathrm{j}\frac{2\pi\Delta R}{\lambda}}a_n(\theta_r)\right)+\\&w_n(t)=\hat{s}(t)\left(a_n(\theta_d)+\rho\mathrm{e}^{-\mathrm{j}\frac{2\pi\Delta R}{\lambda}}a_n(\theta_r)\right)+w_n(t)\end{aligned} \tag{7}$$

where $s'(t)=\xi g(t-\tau_0)\mathrm{e}^{\mathrm{j}(2\pi f_0(t-\tau_0)+\varphi)}$, $\hat{s}(t)=\left(1+\rho\mathrm{e}^{-\mathrm{j}\frac{2\pi\Delta R}{\lambda}}\right)s'(t)$, $a_n(\theta_r)=\mathrm{e}^{\mathrm{j}2\pi\frac{(n-1)d\sin\theta_r}{\lambda}}$, and $d_n=(n-1)d$ $(n=1,2,\cdots,N)$.

Arrange the receiving signals of all the elements into a vector, and we have

$$\begin{aligned}&\boldsymbol{X}(t)=[x_1(t),x_2(t),\cdots,x_N(t)]^{\mathrm{T}}=\\&[\boldsymbol{A}(\theta_d),\boldsymbol{A}(\theta_r)]\begin{bmatrix}1\\ \rho\mathrm{e}^{-\mathrm{j}\frac{2\pi\Delta R}{\lambda}}\end{bmatrix}\hat{s}(t)+\boldsymbol{W}(t)=\\&\boldsymbol{A}(\theta_d,\theta_r)\hat{s}(t)+\boldsymbol{W}(t)\end{aligned} \tag{8}$$

where

$$\begin{aligned}&\boldsymbol{A}(\theta_d,\theta_r)=[\boldsymbol{A}(\theta_d),\boldsymbol{A}(\theta_r)]\begin{bmatrix}1\\ \rho\mathrm{e}^{-\mathrm{j}\frac{2\pi\Delta R}{\lambda}}\end{bmatrix}=\\&\boldsymbol{A}(\theta_d)+\rho\mathrm{e}^{-\mathrm{j}\frac{2\pi\Delta R}{\lambda}}\boldsymbol{A}(\theta_r).\end{aligned} \tag{9}$$

In (9), $\boldsymbol{A}(\theta_d)$ is the steering vector of the direct wave and $\boldsymbol{A}(\theta_r)$ is the steering vector of the reflected wave. $\boldsymbol{W}(t)$ is the noise vector of the array. These vectors can be written as

$$\boldsymbol{A}(\theta_d)=\left[\ a_1(\theta_d),a_2(\theta_d),\cdots,a_N(\theta_d)\ \right]^{\mathrm{T}}, \tag{10}$$

$$\boldsymbol{A}(\theta_r)=[a_1(\theta_r),a_2(\theta_r),\cdots,a_N(\theta_r)]^{\mathrm{T}}, \tag{11}$$

$$\boldsymbol{W}(t)=[w_1(t),w_2(t),\cdots,w_N(t)]^{\mathrm{T}}. \tag{12}$$

3. Robust joint estimation method

After down-conversion and matched filtering of the received signal, (8) can be rewritten as

$$\boldsymbol{X}'(t)=[\boldsymbol{A}(\theta_d),\boldsymbol{A}(\theta_r)]\begin{bmatrix}1\\ \rho\mathrm{e}^{-\mathrm{j}\frac{2\pi\Delta R}{\lambda}}\end{bmatrix}\gamma\mathrm{psf}(t-\tau_0)\mathrm{e}^{\mathrm{j}2\pi f_d t}+\boldsymbol{W}'(t) \tag{13}$$

where t is the time in the distance dimension and $t=mT+k/f_s$ $(k=1,2,\cdots,K;m=1,2,\cdots,M)$. m is the number of pulses and k is the sampling point. f_s is the sampling rate in the distance dimension, K is the sampling number in the distance dimension, T is the pulse repetition period, and M is the pulse number in the coherent processing interval (CPI). psf$(\cdot)$ is the point spread function, which can be seen as a sinc function for the linear frequency modulation (LFM) signal. γ is the complex coefficient of the target signal after pulse compression. f_d is the Doppler frequency of the target. Aircraft or missiles can be regarded as point targets for narrowband surveillance radar. In the stage of the target tracking, τ_0 and f_d are obtained.

$\boldsymbol{X}'$ is a three-dimension data matrix. For each pulse, the dimension of the received data in $\boldsymbol{X}'$ is $N\times K$. We choose the column of the received data according to τ_0 for each pulse, i.e., the range cell of the target. Take all the data of the M pulses at the time τ_0 from $\boldsymbol{X}'$ and form a matrix $\boldsymbol{Y}$, whose dimension is $N\times M$.

Define a vector $\boldsymbol{\beta}$, it can be thought as a compound reflection coefficient vector.

$$\boldsymbol{\beta}=\begin{bmatrix}1\\ \rho\mathrm{e}^{-\mathrm{j}\frac{2\pi\Delta R}{\lambda}}\end{bmatrix}\gamma \tag{14}$$

The mth snapshot vector of $\boldsymbol{Y}$ is

$$\begin{aligned}&\boldsymbol{Y}(m)=[\boldsymbol{A}(\theta_d),\boldsymbol{A}(\theta_r)]\boldsymbol{\beta}\mathrm{e}^{\mathrm{j}2\pi f_d mT}+\boldsymbol{W}'(mT)=\\&\boldsymbol{F}(\theta_d,\theta_r)\boldsymbol{\beta}\mathrm{e}^{\mathrm{j}2\pi f_d mT}+\boldsymbol{W}'(mT)\end{aligned} \tag{15}$$

where $\boldsymbol{F}(\theta_d,\theta_r)=[\boldsymbol{A}(\theta_d),\boldsymbol{A}(\theta_r)]$.

Define a vector $\boldsymbol{\eta}$ consisting the unknown parameters

$$\boldsymbol{\eta}=[\theta_d,\theta_r]. \tag{16}$$

The joint probability density function of the received

data can be expressed as

$$f(\boldsymbol{Y}(1),\boldsymbol{Y}(2),\cdots,\boldsymbol{Y}(M)|\boldsymbol{\eta},\boldsymbol{\beta}) = \prod_{m=1}^{M}\frac{1}{\pi^N\sigma^{2N}}\mathrm{e}^{-\frac{1}{\sigma^2}\left|\boldsymbol{Y}(m)-\boldsymbol{F}(\boldsymbol{\eta})\boldsymbol{\beta}\mathrm{e}^{\mathrm{j}2\pi f_d mT}\right|^2} \tag{17}$$

where σ is the noise standard deviation.

Ignoring the constant, the logarithmic likelihood function is

$$Z(\boldsymbol{\eta},\boldsymbol{\beta}) = -MN\ln\sigma^2 - \frac{1}{\sigma^2}\sum_{m=1}^{M}\left|\boldsymbol{Y}(m)-\boldsymbol{F}(\boldsymbol{\eta})\boldsymbol{\beta}\mathrm{e}^{\mathrm{j}2\pi f_d mT}\right|^2. \tag{18}$$

Take the derivative of (18) with respect to σ, we have

$$\frac{\partial Z(\boldsymbol{\eta},\boldsymbol{\beta})}{\partial\sigma} = -MN\frac{2}{\sigma} + \frac{2}{\sigma^3}\sum_{m=1}^{M}\left|\boldsymbol{Y}(m)-\boldsymbol{F}(\boldsymbol{\eta})\boldsymbol{\beta}\mathrm{e}^{\mathrm{j}2\pi f_d mT}\right|^2. \tag{19}$$

The estimation of the noise power is

$$\hat{\sigma}^2 = \frac{1}{MN}\sum_{m=1}^{M}\left|\boldsymbol{Y}(m)-\boldsymbol{F}(\boldsymbol{\eta})\boldsymbol{\beta}\mathrm{e}^{\mathrm{j}2\pi f_d mT}\right|^2. \tag{20}$$

Substitute (20) into (18), then we have

$$Z(\boldsymbol{\eta},\boldsymbol{\beta}\left|\sigma=\hat{\sigma}\right.) = -MN\ln\frac{1}{MN}\cdot\sum_{m=1}^{M}\left|\mathbf{Y}(m)-\mathbf{F}(\eta)\boldsymbol{\beta}\mathrm{e}^{\mathrm{j}2\pi f_d mT}\right|^2 - MN = -MN\ln\frac{1}{MN}\sum_{m=1}^{M}\boldsymbol{G}^{\mathrm{H}}\boldsymbol{G} - MN \tag{21}$$

where $\boldsymbol{G} = \boldsymbol{Y}(m)-\boldsymbol{F}(\boldsymbol{\eta})\boldsymbol{\beta}\mathrm{e}^{\mathrm{j}2\pi f_d mT}$.

Let

$$Q(\boldsymbol{\eta},\boldsymbol{\beta}) = \frac{1}{M}\sum_{m=1}^{M}\boldsymbol{G}^{\mathrm{H}}\boldsymbol{G}. \tag{22}$$

Obviously, we can obtain the largest value of $Z(\eta,\beta)$ by minimizing $Q(\boldsymbol{\eta},\boldsymbol{\beta})$.

Expanding (22), we have

$$\begin{aligned}Q(\boldsymbol{\eta},\boldsymbol{\beta}) = {}& \frac{1}{M}\sum_{m=1}^{M}\boldsymbol{Y}^{\mathrm{H}}(m)\boldsymbol{Y}(m) - \frac{1}{M}\sum_{m=1}^{M}\boldsymbol{Y}^{\mathrm{H}}(m)\boldsymbol{F}(\boldsymbol{\eta})\boldsymbol{\beta}\mathrm{e}^{\mathrm{j}2\pi f_d mT} - \\ & \frac{1}{M}\sum_{m=1}^{M}\boldsymbol{\beta}^{\mathrm{H}}\boldsymbol{F}^{\mathrm{H}}(\boldsymbol{\eta})\boldsymbol{Y}(m)\mathrm{e}^{-\mathrm{j}2\pi f_d mT} + \\ & \frac{1}{M}\sum_{m=1}^{M}(\boldsymbol{F}(\boldsymbol{\eta})\boldsymbol{\beta}\mathrm{e}^{\mathrm{j}2\pi f_d mT})^{\mathrm{H}}(\boldsymbol{F}(\boldsymbol{\eta})\boldsymbol{\beta}\mathrm{e}^{\mathrm{j}2\pi f_d mT}) = \\ & \mathrm{E}(\boldsymbol{Y}^{\mathrm{H}}(m)\boldsymbol{Y}(m)) - \mathrm{E}(\boldsymbol{Y}^{\mathrm{H}}(m)\mathrm{e}^{\mathrm{j}2\pi f_d mT})\boldsymbol{F}(\boldsymbol{\eta})\boldsymbol{\beta} - \\ & \boldsymbol{\beta}^{\mathrm{H}}\boldsymbol{F}^{\mathrm{H}}(\boldsymbol{\eta})E(\boldsymbol{Y}(m)\mathrm{e}^{-\mathrm{j}2\pi f_d mT}) + \boldsymbol{\beta}^{\mathrm{H}}\boldsymbol{F}^{\mathrm{H}}(\boldsymbol{\eta})\boldsymbol{F}(\boldsymbol{\eta})\boldsymbol{\beta}.\end{aligned} \tag{23}$$

The ML estimation of $\boldsymbol{\beta}$ can be written as

$$\boldsymbol{\beta} = \left(\boldsymbol{F}^{\mathrm{H}}(\boldsymbol{\eta})\boldsymbol{F}(\boldsymbol{\eta})\right)^{-1}\boldsymbol{F}^{\mathrm{H}}(\boldsymbol{\eta})\mathrm{E}\left(\boldsymbol{Y}(m)\mathrm{e}^{-\mathrm{j}2\pi f_d mT}\right). \tag{24}$$

Substituting (24) into (23), we have

$$\begin{aligned}Q(\boldsymbol{\eta}) = {}& \mathrm{E}(\boldsymbol{Y}^{\mathrm{H}}(m)\boldsymbol{Y}(m)) - \mathrm{E}(\boldsymbol{Y}^{\mathrm{H}}(m)\mathrm{e}^{\mathrm{j}2\pi f_d mT})\boldsymbol{F}(\boldsymbol{\eta})\times \\ & (\boldsymbol{F}^{\mathrm{H}}(\boldsymbol{\eta})\boldsymbol{F}(\boldsymbol{\eta}))^{-1}\boldsymbol{F}^{\mathrm{H}}(\boldsymbol{\eta})\mathrm{E}(\boldsymbol{Y}(m)\mathrm{e}^{-\mathrm{j}2\pi f_d mT}).\end{aligned} \tag{25}$$

Then one can obtain the ML estimation of h_t.

$$\begin{aligned}h_t = {}& \arg\max_{h_t}(\mathrm{E}(\boldsymbol{Y}(m)\mathrm{e}^{-\mathrm{j}2\pi f_d mT})^{\mathrm{H}}\boldsymbol{F}(\boldsymbol{\eta})\times \\ & (\boldsymbol{F}^{\mathrm{H}}(\boldsymbol{\eta})\boldsymbol{F}(\boldsymbol{\eta}))^{-1}\boldsymbol{F}^{\mathrm{H}}(\boldsymbol{\eta})\mathrm{E}(\boldsymbol{Y}(m)\mathrm{e}^{-\mathrm{j}2\pi f_d mT})).\end{aligned} \tag{26}$$

We need a two-dimension variable search for $\boldsymbol{\eta}$ and the computation burden is large.

According to Fig. 1 and (4), we can obtain

$$\theta_r = \arccos\left(\frac{R_0\cos\theta_d}{\sqrt{R_0^2+4(R_0\sin\theta_d+h_a-h_g)(h_a-h_g)}}\right), \tag{27}$$

$$\theta_d = \arcsin\left(\frac{h_t-h_a}{R_0}\right). \tag{28}$$

Here h_a can be measured, and h_g can be obtained by the digital elevation model (DEM). At the stage of the target tracking, R_0 has been obtained. Then θ_d and θ_r are only the function of h_t according to (27) and (28). $\boldsymbol{F}(\boldsymbol{\eta})$, the generalized steering vector, can be represented as the functions of h_t too. The computational complexity of the proposed algorithm focuses on (26) from which we can see that the main computation is the multiplication and inversion of the matrix. It can be also seen that the inverse matrix is a 2×2 matrix and the computation cost is very low. Moreover, since we change two-dimension variable search into one-dimension variable search, the computation burden of the proposed algorithm can be reduced a lot compared with the conventional ML method.

Although the DEM has several meters error, we just use h_g from DEM to obtain the geometric relationship between θ_d and θ_r in (27) and we do not use the phase relationship between the direct and multipath echoes. It has little effect on the height estimation precision. Because the proposed method uses the echo data to estimate the compound reflection coefficient, it is insensi-tive to the errors of reflecting surface height and ground specular reflection coefficient.

The flowchart of the proposed algorithm is shown in Fig. 2. We obtain $\boldsymbol{X}'(t)$ after down-conversion and matched filtering of the received signal, then extract the target range cell data from $\boldsymbol{X}'(t)$ to form the matrix $\boldsymbol{Y}$. According to (27) and (28), the generalized steering vector $\boldsymbol{F}(\boldsymbol{\eta})$ can only be represented as the functions of h_t. Meanwhile, Doppler frequency of the target f_d can be

calculated from the radar tracking filter. Finally, the target height can be estimated using (26) with one-dimension search.

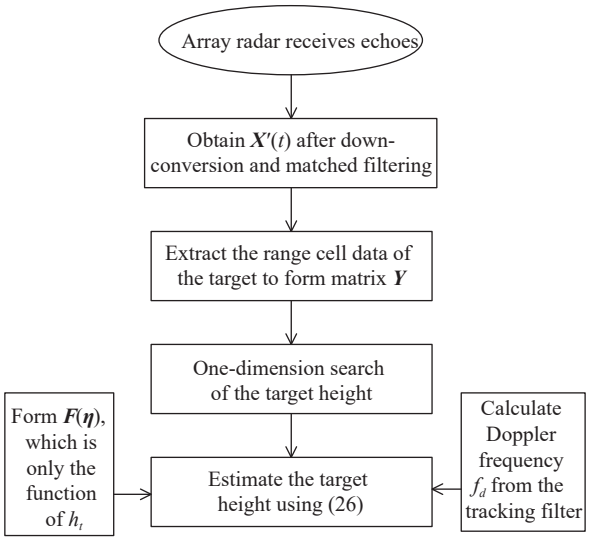

Fig. 2 Flowchart of the proposed method

4. Simulation and experiment results

Consider a vertical uniform linear digital array radar with 20 elements. The radar works in the meter band and the inter-element distance is $\lambda/2$. The distance from the radar to the target is 12 km. The reflecting surface height is −6 m and the height of radar is 8 m. The ground reflection coefficient is assumed to be $0.95e^{j\frac{17}{18}\pi}$ and the target height is 460 m. Monte Carlo simulation has been carried out and its number is 500. The root mean square error (RMSE) is used to represent the estimation performance of the target height.

The RMSE performance of the target height against the signal to noise ratio (SNR) is shown in Fig. 3. Since the proposed joint estimation method utilizes the relationship between the direct wave and the multipath reflected wave, the performance of the proposed robust joint estimation mthod is superior to that of the conventional ML method.

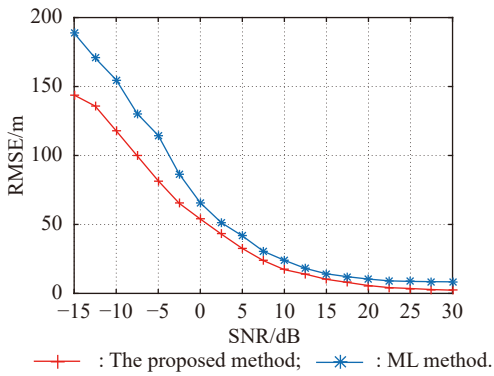

Fig. 3 Estimation performance against SNR

The influence of the reflecting surface height error on the proposed method is shown in Fig. 4. It can be observed that the reflecting surface height error has little effect on the proposed method because we do not use the reflecting surface height as a known parameter to obtain the phase relationship between the direct and multipath echoes, and then the proposed method has good robustness to the reflecting surface height error.

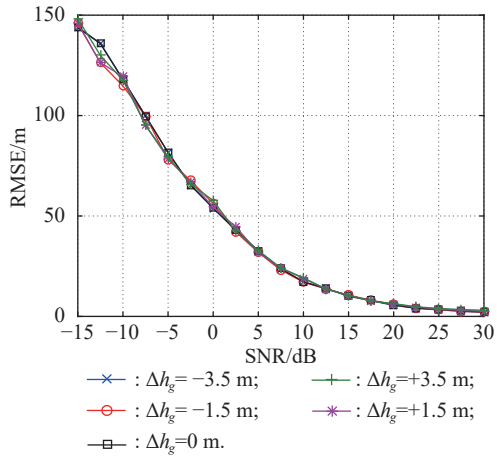

Fig. 4 Estimation performance of the proposed method with reflecting surface height errors

The two methods' estimation performance with reflecting surface height errors are compared in Fig. 5. It can be observed that the estimation accuracy of the highly deterministic ML method is closely related to the reflecting surface height error. When there is no error of the reflecting surface height, the highly deterministic ML method has better performance. The height of the reflecting surface can hardly be measured accurately, because the position of the reflecting point varies with the target range or height. When the height of the reflecting surface cannot be obtained accurately, the estimation accuracy of the highly deterministic ML method will decrease sharply. From Fig. 5, it can also be observed that the highly deterministic ML method has an error floor with increasing SNR. That is because noise no longer plays a leading role for the estimation performance at high SNRs. And the reflecting surface height error causes a fixed estimation error which is larger than that of the noise. In the proposed joint estimation method, the reflecting surface height error and the ground reflection coefficient error are included in the compound reflection coefficient which is estimated based on the echo data. Thus the proposed joint estimation method is insensitive to the reflecting surface height error.

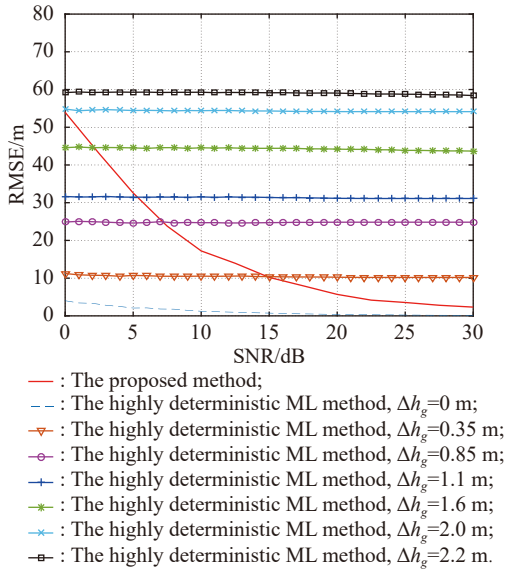

Fig. 5 Estimation performance comparison with the highly deterministic ML method

We also analyze the effect of the target velocity change on the performance of the proposed method in Fig. 6. The RMSEs of the target height under different SNRs are compared. It can be seen that several meters per second velocity error or change has little effect on the performance of the proposed method. Thus the proposed method has good robustness to target velocity changes. In fact, it is difficult to keep the target moving at a uniform radial velocity against radar.

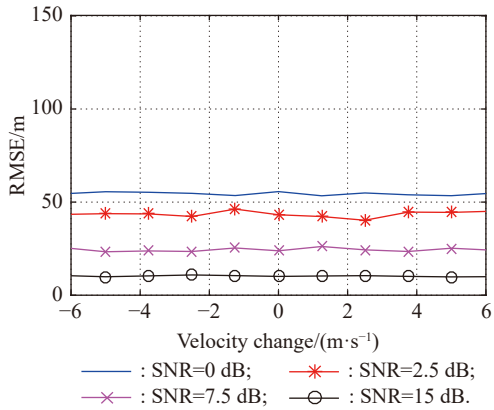

Fig. 6 Estimation performance of the proposed method with velocity change against SNR

When the target gains acceleration, the RMSE performance versus SNR is shown in Fig. 7. We observe that the acceleration of the target has little effect on the estimation performance of the target height. It is because the velocity change caused by the acceleration is small in a short CPI time.

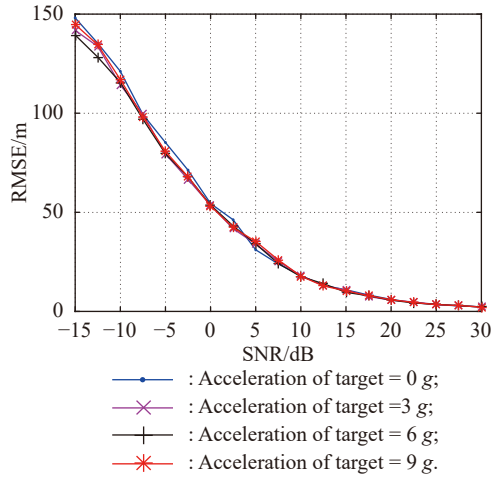

Fig. 7 Estimation performance of the proposed method with acceleration against SNR

The influences of the ground specular reflection coefficient error on the performances of the proposed method and the highly deterministic ML method are shown in Fig. 8. It can be observed that the phase error of the ground specular reflection coefficient has great influence on the highly deterministic ML method. When the phase of the ground specular reflection coefficient is consistent with the true value, the highly deterministic ML method has high estimation accuracy. When there is an error between the phases of the real ground specular reflection coefficient and that used in the simulation model, the per-for-mance of the highly deterministic ML method is obviously deteriorated. Moreover, the estimation accuracy of the highly deterministic ML method cannot be further improved with increasing SNR. That is because the simulation model does not match with the real scenario accurately and a fixed error occurs. Since the proposed method uses the echo data to estimate the compound reflection coefficient and do not use the specular reflection coefficient directly, the proposed method is robust to the ground reflection coefficient error.

Finally, the practical data processing results of the proposed joint estimation method are presented. The data comes from a meter band uniform linear digital array early warning radar with 20 elements and the interelement distance being 0.6λ. The reflecting surface height of a lake is 4 m and the radar center height is 10 m. A plane as a target flies at the altitude of 7−8 km with an approximately uniform velocity. The direct distance from the radar to the target is from 200 km to 250 km. For the far distance target, we have considered the effect of the curvature of the earth in the processing and therefore the

plane can be thought as the low-angle target. From Fig. 9, it can be seen that the processing result of the proposed met-hod is better than that of the conventional ML method.

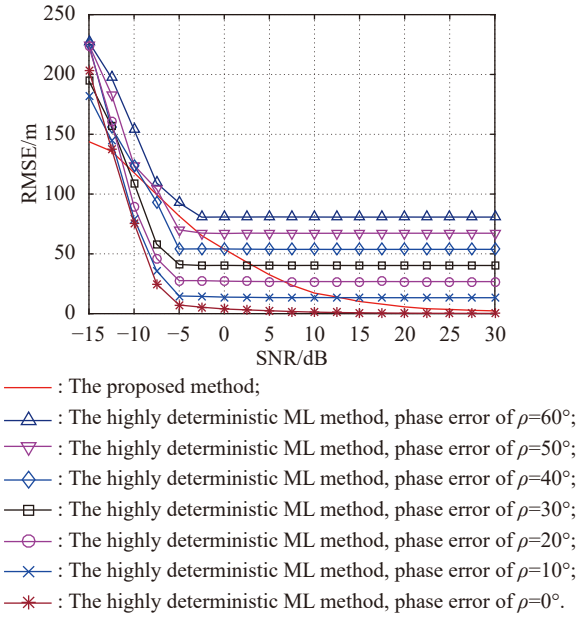

Fig. 8 Estimation performance when the amplitude error of ρ is 0.1 with different phase errors

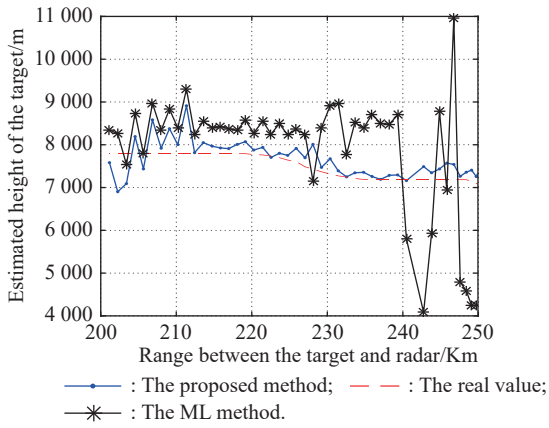

Fig. 9 Experiment data processing results

In Fig. 10, the proposed joint estimation method has better performance in real data processing. The estimation result of the highly deterministic ML method without the reflecting surface height error is very close to the true value. When the reflecting surface height error is 1.5 m or more, the accuracy of the highly deterministic ML method is too poor to be used for the high-precision measurement radar.

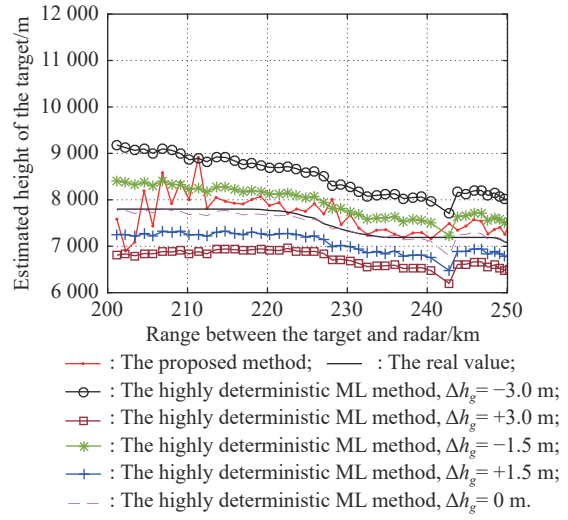

Fig. 10 Experiment data processing results with reflecting surface height errors

5. Conclusions

In this paper, a robust low-angle target height estimation method is proposed based on the compound reflection coefficient multipath model. The proposed method uses the echo data to obtain the compound reflection coefficient, and set up one-dimension generalized steering vector to estimate the target height. Thus it is robust to the reflecting surface height error and the ground reflection coefficient error. Moreover, the computation burden of the proposed algorithm is low for its one-dimension variable search. At last, the simulation and experiment results demonstrate the validity of the proposed method.

References

[1] YE W, ZHU A H, FAN H D. Survey of route planning of low altitude penetration. Journal of System Simulation, 2007, 19(10): 2357–2361. (in Chinese)

[2] SHADDRACK Y N, CHEN H, WANG W Q. OFDM chirp radar for adaptive target detection in low grazing angle. IET Signal Processing, 2018, 12(5): 613–619.

[3] HU Z Z, XU K H, SHEN C L. Digital map information fusion in low altitude penetration system. Journal of Nanjing University of Aeronautics & Astronautics, 2000, 32(4): 434–438. (in Chinese)

[4] WANG S H, CAO Y H, SU H T. Target and reflecting surface height joint estimation in low-angle radar. IET Radar, Sonar and Navigation, 2016, 10(3): 617–623.

[5] LI C X, CHEN B X, ZHENG Y S, et al. Altitude measurement of low elevation target in complex terrain based on orthogonal matching pursuit. IET Radar, Sonar and Navigation, 2017, 11(5): 745–751.

[6] ZENG X L, YANG M L, CHEN B X, et al. Estimation of direction of arrival by time reversal for low-angle targets. IEEE Trans. on Aerospace and Electronic Systems, 2018, 54(6): 2675–2694.

[7] BOSSE E, TURNER R M, RISEBOROUGH E S. Model-based multifrequency array signal processing for low-angle tracking. IEEE Trans. on Aerospace and Electronic Systems, 1995, 31(1): 194–210.

[8] BONACCI D, VINCENT F, GIGLEUX B. Robust DOA estimation in case of multipath environment for a sense and avoid airborne radar. IET Radar, Sonar and Navigation, 2017, 11(5): 797–801.
[9] KIM J, YANG H J, KWAK N. Low-angle tracking of two objects in a three-dimensional beamspace domain. IET Radar, Sonar and Navigation, 2012, 6(1): 9–10.
[10] ZHENG Y S, CHEN B X. Multipath model and inversion method for low-angle target in very high frequency radar. Journal of Electronics and Information Technology, 2016, 38(6): 1468–1474. (in Chinese)
[11] WHITE W D. Low-angle radar tracking in the presence of multipath. IEEE Trans. on Aerospace Electronic Systems, 1974, 10(6): 835–852.
[12] CAO Y H, ZHANG Z J, WANG S H, et al. Direction finding for bistatic MIMO radar with uniform circular array. International Journal of Antennas and Propagation, 2013. DOI: 10.1155/2013/674878.
[13] LIU M B, HU G P, SHI J P, et al. DOA estimation method for multi-path targets based on TR MIMO radar. The Journal of Engineering, 2019(2): 461–465.
[14] LIU Y, JIU B, XIA X G, et al. Height measurement of low-angle target using MIMO radar under multipath interference. IEEE Trans. on Aerospace and Electronic Systems, 2018, 54(2): 808–818.
[15] ZHENG Y, YU Y Z. Joint estimation of DOA and TDOA of multiple reflections by matrix pencil in mobile communications. IEEE Access, 2019, 7: 15469–15477.
[16] BLAIR W D, BRANDT-PEARCE M. Statistics of monopulse measurements for tracking targets in the presence of sea-surface induced multipath. IEEE Aerospace Applications Conference Proceedings, 1998, 1: 49–58.
[17] BAR S Y, KUMAR A, BLAIR W D, et al. Tracking low elevation targets in the presence of multipath propagation. IEEE Trans. on Aerospace and Electronic Systems, 1994, 30(3): 973–979.
[18] DAEIPOUR E, BLAIR W D, BAR S Y. Bias compensation and tracking with monopulse radars in the presence of multi path. IEEE Trans. on Aerospace and Electronic Systems, 1997, 33(3): 863–882.
[19] YAN F G, JIN M, LIU S, et al. Real-valued MUSIC for efficient direction estimation with arbitrary arraygeometries. IEEE Trans. on Signal Processing, 2014, 62(6): 1548–1560.
[20] LIU Z, WANG Y Y, CAO Y H. Real-domain GMUSIC algorithm based on unitary-transform for low-angle estimation. Journal of Systems Engineering and Electronics, 2014, 25(5): 794–799.
[21] ROY R, KAILATH T. ESPRIT-estimation of signal parameters via rotational invariance techniques. IEEE Trans. on Acoustics, Speech, and Signal Processing, 1989, 37(7): 984–995.
[22] LI C C, LIAO G S, ZHU S Q, et al. An ESPRIT-like algorithm for coherent DOA estimation based on data matrix decomposition in MIMO radar. Signal Processing, 2011, 91(8): 1803–1811.
[23] SUN M, CEDRIC L B, WANG Y D, et al. Time delay estimation using ESPRIT with extended improved spatial smoothing techniques for radar signals. IEEE Geoscience Remote Sensing Letters, 2016, 13(1): 73–77.
[24] CHEN D F, CHEN B X, QIN G D. Angle estimation using ESPRIT in MIMO radar. Electronics Letters, 2008, 44(12): 770–771.
[25] RAO B D, HARI K V S. Weighted subspace methods and spatial smoothing: analysis and comparison. IEEE Trans. on Signal Processing, 1993, 41(2): 788–803.
[26] ZHU Y T, ZHAO Y B, SHUI P L. Low-angle target tracking using frequency-agile refined maximum likelihood algorithm. IET Radar, Sonar and Navigation, 2017, 11(3): 491–497.
[27] LI J. Improved angular resolution for spatial smoothing techniques. IEEE Trans. on Signal Processing, 1992, 40(12): 3078–3081.
[28] BOMAN K, STOICA P. Low angle estimation: models, methods, and bounds. Digital Signal Processing, 2001, 11(1): 35–79.
[29] LO T, LITVA J. Use of a highly deterministic multipath signal model in low-angle tracking. IEEE Proceeding of Radar Signal Processing, 1991, 138(2): 163–171.
[30] HEINER K. VHF/UHF radar part 1: characteristics. Electronics & Communication Engineering Journal, 2002, 14(2): 61–72.
[31] HEINER K. VHF/UHF radar part 2: operational aspects and applications. Electronics & Communication Engineering Journal, 2002, 14(3): 101–111.
[32] ZHANG Y S, GUO Y D, NIU X L, et al. Angle estimation of coherent multi-target for MIMO bistatic radar. Proc. of the International Conference on Image Analysis and Signal Processing, 2010: 146–149.

Biographies

WANG Shenghua was born in 1979. She received her Ph.D. degree in information and communication engineering from Xidian University, Xi' an, China, in 2019. She joined Xi'an University of Posts and Telecommunications, Xi 'an, China in 2019. Her research interests include array signal processing, radar signal processing integrated with communication, and low angle radar systems.
E-mail: wshh_2011@163.com

CAO Yunhe was born in 1978. He received his B.S. degree in measuring control and instrument engineering in 2001, and M.S. and Ph.D. degrees in electrical engineering from Xidian University, Xi'an, China, in 2004 and 2006, respectively. He is a professor in Xidian University. His research interests include array signal processing, MIMO radar, and wideband radar signal processing.
E-mail: cyh_xidian@163.com

LIU Yutao was born in 1981. He received his Ph.D. degree in communication engineering from Harbin Institute of Technology, Harbin, China. His research interests include communication signal processing, and radar signal processing integrated with communication.
E-mail: yutaoliu2020@163.com